J Neuropathol Exp Neurol
Vol. 67, No. 11
November 2008
pp. 1063–1071

ORIGINAL ARTICLE

Nonviral DNA Vaccination Augments Microglial Phagocytosis of β-Amyloid Deposits as a Major Clearance Pathway in an Alzheimer Disease Mouse Model

Yoshio Okura, MD, PhD, Kuniko Kohyama, MS, Il-Kwon Park, DVM, PhD, and Yoh Matsumoto, MD, PhD

Abstract

Immunotherapies markedly reduce β-amyloid (Aβ) burden and reverse behavioral impairment in mouse models of Alzheimer disease. We previously showed that new Aβ DNA vaccines reduced Aβ deposits in Alzheimer disease model mice without detectable side effects. Although they are effective, the mechanisms of Aβ reduction by the DNA vaccines remain to be elucidated. Here, we analyzed vaccinated and control Alzheimer disease model mice from 4 months to 15 months of age to assess which of several proposed mechanisms may underlie the beneficial effects of this vaccination. Immunohistochemical analysis revealed that activated microglial numbers increased significantly in the brains of vaccinated mice after DNA vaccination both around Aβ plaques and in areas remote from them. Microglia in treated mice phagocytosed Aβ debris more frequently than they did in untreated mice. Although microglia had an activated morphological phenotype, they did not produce significant amounts of tumor necrosis factor. Amyloid plaque immunoreactivity and Aβ concentrations in plasma increased slightly in vaccinated mice compared with controls at 9 but not at 15 months of age. Collectively, these data suggest that phagocytosis of Aβ deposits by microglia plays a central role in Aβ reduction after DNA vaccination.

Key Words: β-Amyloid, Alzheimer disease, DNA vaccine, Microglia.

INTRODUCTION

Alzheimer disease (AD) is the most common cause of age-related cognitive decline; it affects more than 12 million people worldwide (1). It is widely believed that accumulation of β-amyloid (Aβ) is the first event in the pathogenesis of AD and that it precedes tau phosphorylation, tangle formation, and neuron death (i.e. the amyloid cascade hypothesis) (2). Based on this hypothesis, Schenk et al (3) demonstrated that a vaccine composed of synthetic Aβ in complete Freund adjuvant induced high anti-Aβ antibody titers, leading to dramatic reductions of Aβ deposits in platelet-derived growth factor promoter–expressing amyloid precursor protein (PDAPP) transgenic mice (3). On the basis of these promising results, clinical trials with Aβ peptide (AN-1792) in conjunction with the T helper 1 adjuvant, QS-21, were initiated; however, the clinical trial was halted because some patients developed meningoencephalitis (4). Importantly, neuropathologic examination of treated patients showed apparent clearance of Aβ plaques from large areas of the neocortex (5, 6). Thus, it seems that vaccine therapy could be effective for AD if inflammatory/immune reactions are minimized.

We previously developed nonviral Aβ DNA vaccines with plasmid vectors and succeeded in reducing Aβ burden in APP23 mice without inducing side effects such as neuroinflammation (7). The mechanism of Aβ reduction after DNA vaccination, however, has not yet been elucidated. Three hypotheses explain how anti-Aβ antibodies reduce Aβ deposits in the brain (8, 9). The first is that anti-Aβ antibodies attached to Aβ plaques enhance Fc receptor–mediated phagocytosis of Aβ by microglia (10). The second mechanism is the direct effect of antibodies on Aβ, leading to the dissolution of amyloid fibrils or neutralization of Aβ oligomers (11, 12). Finally, the "peripheral sink hypothesis" postulates that anti-Aβ antibodies in the circulation results in a net efflux of Aβ from the brain into blood vessels (13, 14).

In this study, we examined whether these clearance mechanisms take place in our DNA vaccination system. We found that microglia were activated, increased in number, and phagocytosed Aβ deposits after vaccine administration. The results suggest that phagocytosis of Aβ deposits by activated microglia is a major clearance pathway of Aβ clearance after DNA vaccination and may provide important information for the development of effective new vaccines against AD.

MATERIALS AND METHODS

Animals

APP23 transgenic and wild-type B6 mice were used for analysis; and detailed information was provided in a previous

From the Department of Molecular Neuropathology, Tokyo Metropolitan Institute for Neuroscience, Fuchu, Tokyo, Japan.
Send correspondence and reprint requests to: Yoh Matsumoto, MD, PhD, Department of Molecular Neuropathology, Tokyo Metropolitan Institute for Neuroscience, 2-6 Musashidai, Fuchu, Tokyo, Japan 183-8526; E-mail: matyoh@tmin.ac.jp
This study was supported in part by Health and Labour Sciences Research Grants for Research on Psychiatric and Neurological Diseases and Mental Health and by Grants-in-Aid from the Japan Society for the Promotion of Science. Yoh Matsumoto was also supported by the Welfare and Health Fund of the Tokyo Metropolitan Government.

report (7). Plasma was obtained from mice under deep inhalation anesthesia with ethyl ether via cardiac puncture with heparinized syringes before autopsy. Anesthetized mice were then killed. All procedures of animal experimentation were approved by the ethics committee of the Tokyo Metropolitan Institute for Neuroscience and performed in accordance with institutional guidelines.

Development and Administration of DNA Vaccines

We prepared Aβ DNA vaccines using a PTarget mammalian expression system (Promega, Tokyo, Japan) and injected them into APP23 mice on a weekly and then biweekly basis as used previously (15). Two DNA vaccines were used: immunoglobulin L (IgL)–Aβ vaccine, which possesses the Igκ signal sequence of mouse immunoglobulin to improve the secretion ability, and Aβ-Fc vaccine that has the Fc portion of human immunoglobulin at the 3′ end to maintain stability. APP23 mice received DNA vaccines (100 μg in 100 μL) regularly from 4 months of age, 2 months before amyloid plaque appearance, to the termination of experiments. Mice were killed at 9 and 15 months of age.

Immunohistochemistry

Mice were killed under deep anesthesia, and the brains were removed and immersion fixed in 4% paraformaldehyde. Paraffin-embedded sections were stained with monoclonal antibodies (mAbs) 6F/3D against Aβ8-17 (DAKO, Tokyo, Japan) and Iba-1 for microglia (WAKO, Tokyo, Japan). Sections were pretreated in formic acid for 3 minutes for 6F/3D staining and 0.1% trypsin for 10 minutes at 37°C for Iba-1 staining. After pretreatment, the sections were incubated in the primary mAbs followed by biotinylated horse anti-mouse immunoglobulin G (IgG) and horseradish peroxidase (HRP)–labeled Vectastain Elite ABC kit (Vector, Funakoshi, Tokyo, Japan). Horseradish peroxidase–binding sites were detected in 0.005% diaminobenzidine and 0.01% hydrogen peroxide. For confocal microscopic analysis, fluorescein isothiocyanate anti-mouse IgG and Cy-3 anti-rabbit IgG were used as secondary antibodies for 6F/3D and Iba-1 staining, respectively. The presence or absence of IgG depositions on Aβ plaques was determined by incubation of sections with biotinylated horse anti-mouse IgG followed by HRP-labeled Vectastain Elite ABC kit.

Quantitative Analysis of Aβ Burden and Microglia

β-Amyloid deposits were quantitated in the cerebral cortex and hippocampus according to the method used previously (15). All the procedures were performed by an individual blinded to the experimental conditions. The amyloid load was measured in 10 fields from the cingulate to retrosplenial cortex in the left hemisphere per mouse. Each field measured 600 × 400 μm and was randomly chosen. Analysis of the entire hippocampus was performed in a similar manner. β-Amyloid deposits that occupied the field were expressed as pixels using National Institutes of Health (NIH) image software.

After Iba-1 staining, the densities of microglia were determined by counting them in randomly selected 10 fields (600 × 400 μm each) from the cingulate to retrosplenial cortex in the left hemisphere of mice (n = 4–6 in each group). Microglia around the plaque (periplaque area) and those remote from the plaque (remote area) were counted separately and expressed as the mean ± SE per field. Using double-stained sections for Aβ and microglia, the densities of phagocytosing microglia were determined in a similar manner under confocal microscopy.

Western Blotting

Brain tissues were homogenized and sonicated in 10 volumes of Tris-buffered saline buffer in the presence of protease inhibitors. One milliliter of formic acid was added to 300 μg of homogenate in 10 μL. After a brief incubation, formic acid was vacuum dried with an acid-proof vacuum evaporator (miVac DNA, Scrum, Tokyo, Japan). After adding NuPAGE LDS sample buffer (Invitrogen, Tokyo, Japan), the samples were incubated at 70°C for 10 minutes and were run on NuPAGE 12% Bis-Tris gel (Invitrogen) (16). Before electrophoresis, protein concentration of each sample was determined, and the volume for loading was adjusted (equivalent to 40 μg); samples were then transferred to polyvinylidene difluoride membrane (Immobilon-P; Millipore, Tokyo, Japan). After blocking with 10% nonfat milk, the blots were incubated with anti-human Aβ 1–17 antibody (6E10; Cambridge, United Kingdom; 1:100) at 4°C overnight followed by incubation with Trueblot HRP-conjugated anti-mouse IgG (eBioscience, San Diego, CA; 1:1000) for 1 hour. The blots were developed by enhanced chemiluminescence reagents (Immunostar Kit Wako; WAKO) according to the manufacturer's instructions. The density of each band obtained by Western blot analysis was measured with a scanning laser densitometer (GS-700, Bio-Rad, Hercules, CA) and analyzed using the NIH image software.

Real-time Polymerase Chain Reaction

Total RNA was extracted from the indicated tissues using an RNAqueous Kit (Ambion), and complementary DNA was then synthesized by reverse transcription using a High Capacity cDNA Reverse Transcription Kit (Applied Biosystems, Foster City, CA). SYBR Green real-time polymerase chain reactions (PCRs) were performed on an ABI PRISM 7500 sequence detection system (Applied Biosystems) in a total volume of 25 μL using the SYBR Premix Ex Taq (Takara Bio, Otsu, Japan). Each PCR was performed in duplicate using thermocycler conditions: Stage 1, 95°C for 10 minutes for 1 cycle and Stage 2, 95°C for 15 seconds and 58°C for 1 minute for 50 cycles. All primers were designed on an intron-exon junction to prevent coamplification of genomic DNA, and their sequences were shown in previous reports (17, 18). Relative quantification of messenger RNA (mRNA) was performed using the standard curve method. Glyceraldehyde-3-phosphate dehydrogenase was used as internal control. The absence of nonspecific amplification was confirmed by dissociation curve analysis.

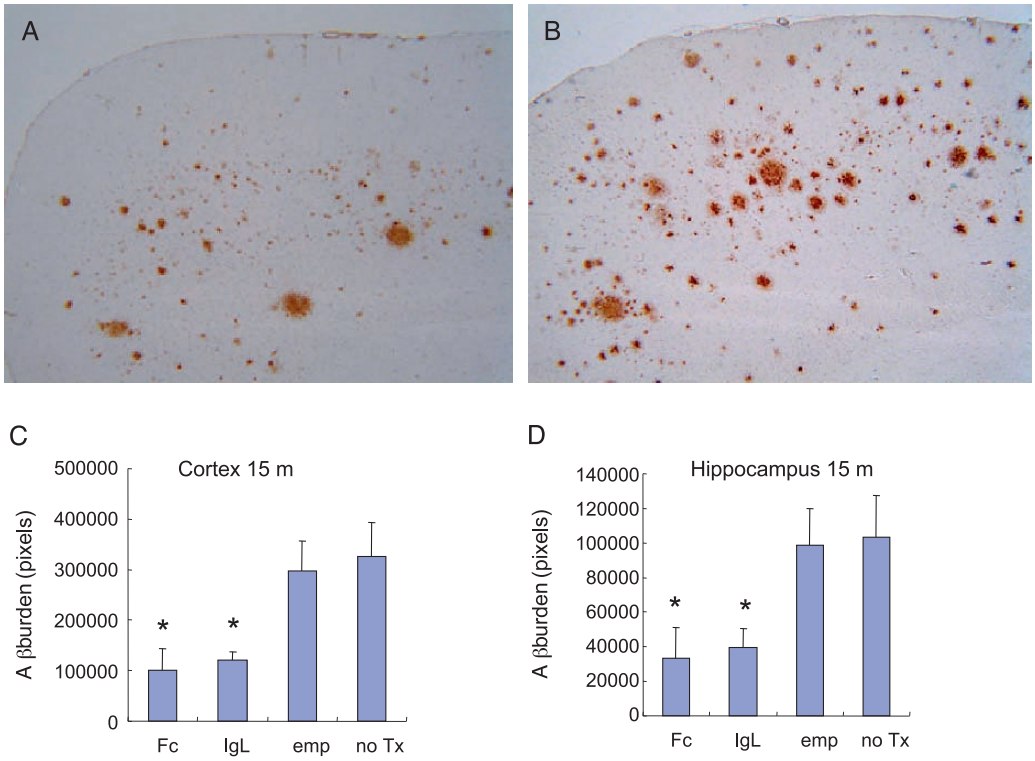

FIGURE 1. β-Amyloid (Aβ) reduction after DNA vaccination in mice at 15 months of age. There were fewer Aβ deposits in the frontal cortex of a mouse that had been treated with the Aβ-Fc vaccine **(A)** than in frontal cortex of a control mouse **(B)**. Semiquantitative analysis revealed that Aβ deposits were significantly reduced (* = $p < 0.01$) in the cortex of vaccinated mice (30.6% of untreated mice) **(C)**. β-Amyloid deposits in the hippocampus were also significantly reduced (* = $p < 0.01$) after vaccine treatment **(D)**. emp, empty vector; no Tx, untreated.

Tissue Amyloid Plaque Immunoreactivity Assay

Plasma to be tested were diluted to ×100, ×300, ×1,000, and ×3,000, and then applied to formic acid-pretreated APP23 brain sections, followed by incubation with biotinylated horse anti-mouse IgG and HRP-labeled Vectastain Elite ABC kit (Vector). The maximal dilution of plasma that gave positive staining was estimated as the amyloid plaque immunoreactivity titer.

Quantification of Tumor Necrosis Factor in the CNS Tissues and Plasma Aβ With ELISA

Brain tissue was homogenized in lysis buffer, and the supernatant was harvested after centrifugation. Each sample was adjusted to 10 mg/mL. The levels of brain tumor necrosis factor (TNF) and plasma Aβ were determined using the Mouse TNF Instant ELISA (Bender MedSystems, Vienna, Austria) and human Aβ (1–42) ELISA Kit (WAKO),

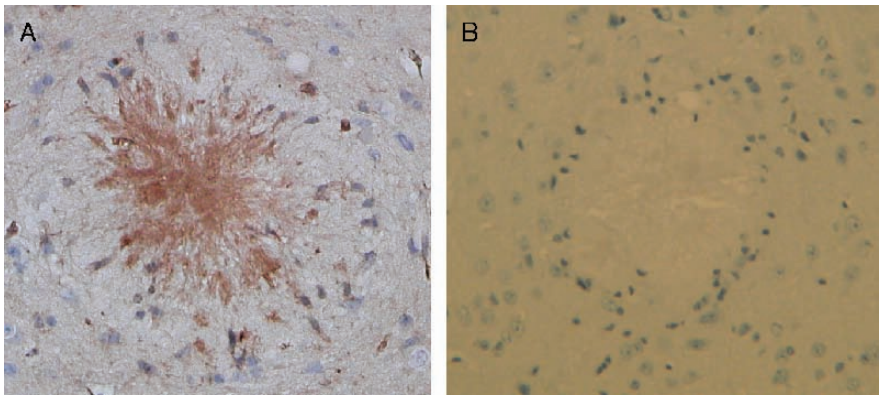

FIGURE 2. Immunoglobulin G (IgG) in the brains of DNA vaccine–treated and untreated APP23 mice at age 15 months. β-Amyloid (Aβ) plaques in the brain of an Aβ-Fc vaccine–treated mouse stained positively for IgG **(A)**, whereas a plaque in an untreated mouse was completely negative **(B)**. Immunohistochemistry with anti-mouse IgG. Original magnification: 200×.

respectively. For positive controls in the TNF assay, 2 types of brain and spinal cord tissue samples were used. For the first type, C57Bl6 mice were given an intraperitoneal injection of 100 μg lipopolysaccharide, and brain tissue was harvested 1 hour later and subjected to ELISA. Second, C57Bl6 mice were immunized twice on Days 0 and 7 with 300 μg of recombinant rat myelin oligodendrocyte protein (MOG) emulsified with complete Freund adjuvant. On Days

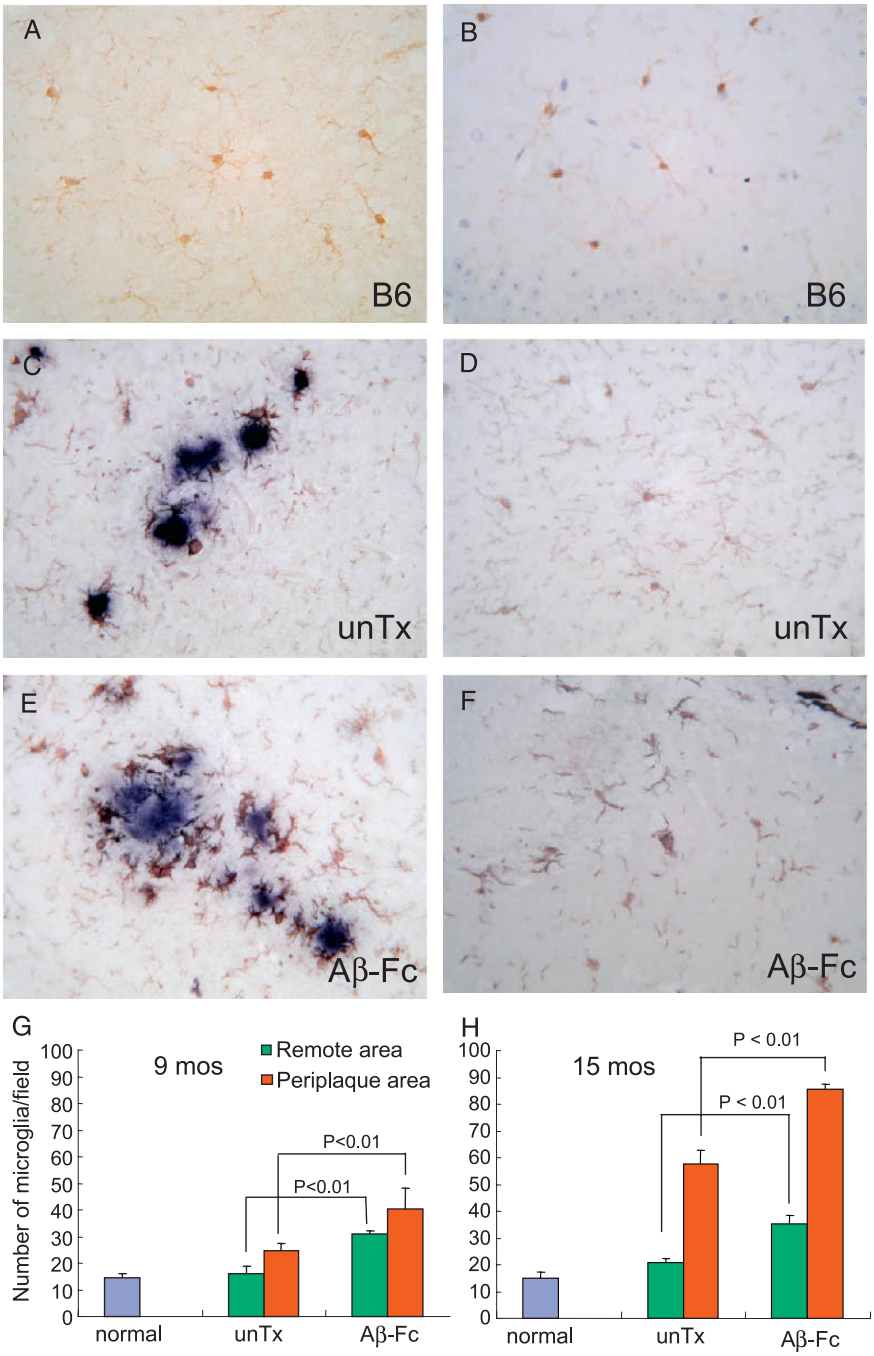

FIGURE 3. Double staining with monoclonal antibodies 6F3D against β-amyloid (Aβ) (blue) and Iba-1 against microglia (brown) of the brains of treated and untreated mice. In normal control B6 mice, ramified resting microglia were sparse in the cortex **(A)** and hippocampus **(B)**. Around plaques of untreated APP23 mice, there were microglia with abundant cytoplasm and processes that had bulbous swellings **(C)**. In areas remote from the plaques in nontreated APP23 mice, resting microglia were sparsely distributed as in control B6 mice **(D)**. In vaccinated mice, more microglia infiltrated amyloid plaques **(E)**. In the area remote from plaques in treated APP23 mice, microglia were more numerous and showed an activated phenotype **(F)**. Semiquantitative analysis was performed at 9 months **(G)** and 15 months **(H)** by counting microglial cell number in 10 fields (3–4 mice per group). Normal, normal B6 mice; unTx, untreated APP23 mice; Aβ-Fc, vaccinated mice.

0 and 2, the mice received intraperitoneal injection of pertussis toxin (300 ng). When they showed complete hind leg paralysis on Day 20 (i.e. clinical experimental autoimmune encephalomyelitis [EAE]), lumbar spinal cords were removed and subject to ELISA analysis.

Statistical Analysis

Student *t*-test or the Mann-Whitney U test was used for the statistical analysis. Values of $p < 0.05$ were considered significant.

RESULTS

DNA Vaccination Reduces Aβ Burden in the Brains of AD Model Mice

We prepared nonviral Aβ DNA vaccines and injected them (100 μg each) into APP23 mice beginning at 4 months of age on a weekly and then biweekly basis (7). At 15 months of age, Aβ deposits were considerably reduced (Figs. 1A, B). Semiquantitative analysis revealed that Aβ deposits in treated mice were reduced to approximately one third of those in nonvaccinated control mice in both the cerebral cortex and hippocampus (Figs. 1C, D).

IgG Deposits Were Detected on Aβ Plaques in the Brains of DNA-Vaccinated, But Not Control Mice

To determine the possible mechanisms of Aβ reduction after DNA vaccination, it was essential to know whether the anti-Aβ antibodies raised by vaccination reach the brain and decorate Aβ plaques. We previously found that the DNA vaccination protocol resulted in a mild but significant induction of anti-Aβ antibodies in plasma in vaccinated mice (7). We performed immunohistochemistry using anti-mouse IgG antibodies to identify IgG on Aβ plaques. Plaques in the brains of treated mice were stained positively for IgG (Fig. 2A), whereas those in untreated mice were completely negative (Fig. 2B). Some cells with morphological features of microglia were also positive for IgG (Fig. 2A). Interestingly, Aβ plaques in empty vector–administered mice were also negative for IgG (data not shown). Thus, antibody binding to the Aβ plaques may occur in the brains of vaccinated mice in vivo.

Microglial Activation and Phagocytosis Induced by DNA Vaccination

We assessed phagocytosis of Aβ deposits by microglia after DNA vaccination. Brain sections from treated and control (i.e. untreated APP23 and wild-type) mice were double-stained with Iba-1 and 6F/3D mAbs. We previously determined that DNA vaccination did not elicit neuroinflammation in either AD model or wild-type mice (7). Because in the present study, Iba-1–positive cells in the CNS showed typical features of resident microglia, they likely were microglia and not macrophages. In untreated B6 mice, ramified microglia with small cytoplasm and fine processes were sparsely distributed throughout the cerebral cortex

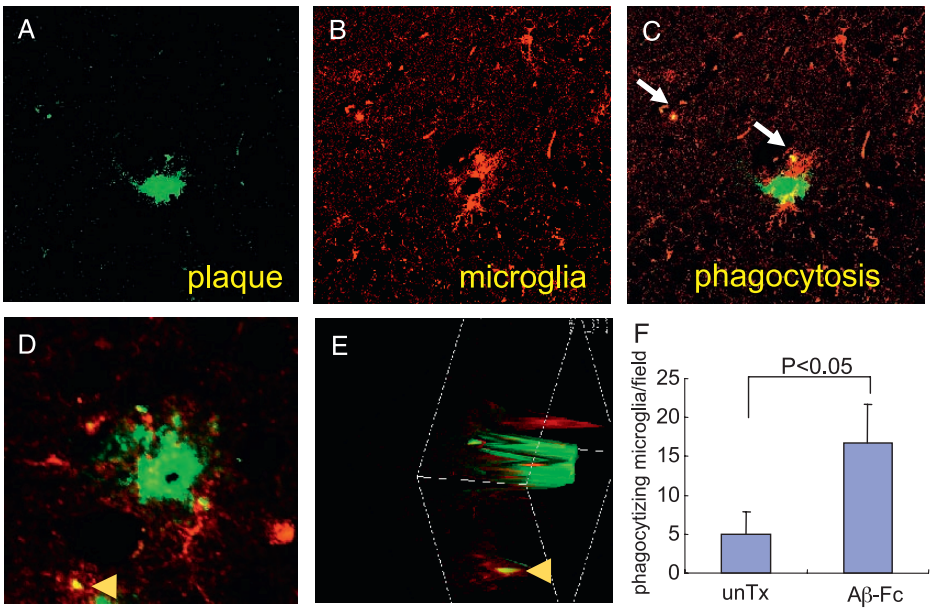

FIGURE 4. Phagocytosis of β-amyloid (Aβ) deposits by activated microglia in the cerebral cortex of mice at 15 months of age. Brain sections from treated **(A–E)** and untreated (not shown) APP23 mice were stained for Aβ with (6F3D, green) **(A)** and for microglia (Iba-1, red) **(B)** monoclonal antibodies and observed with a confocal microscope. Some microglia surrounding the amyloid plaque contained Aβ deposits (C, arrows). Microglia (red) in areas away from Aβ plaques had Aβ staining (**D**, arrowhead) within the cytoplasm. Using 3-dimensional reconstruction, a different plane of the view was shown in (**E**). The Aβ deposit ingested by a microglial cell was indicated by an arrowhead in **(E)**. Semiquantitative analysis revealed that the number of phagocytosed Aβ deposits increased approximately 2.5-fold in treated compared with untreated mice ([**F**] $p < 0.05$). Phagocytosed particles in 10 fields from 4 treated and 4 control mice (total, 40 fields in each group) were counted and compared.

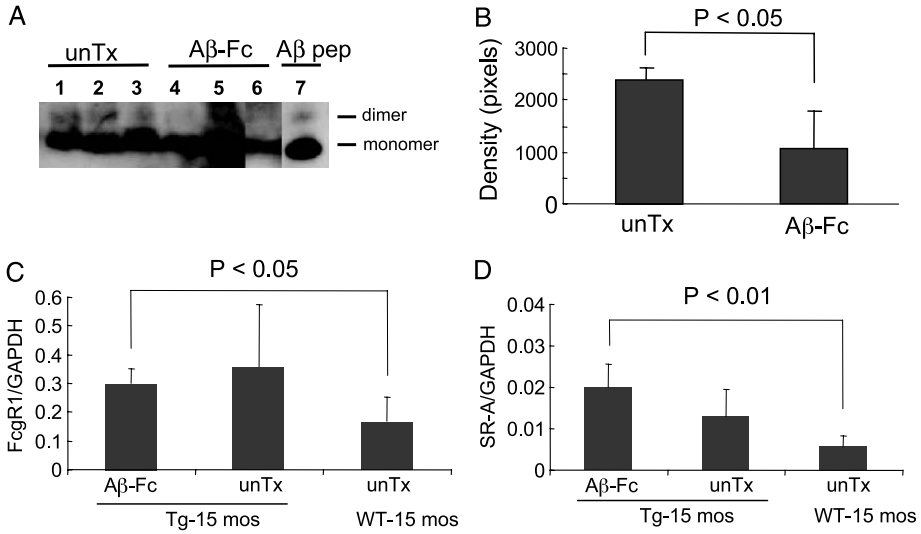

FIGURE 5. Western blot analysis **(A)** demonstrated that β-amyloid (Aβ) monomers plus dimers were reduced after DNA vaccination. Measurements of band densities revealed a statistically significant difference between vaccinated and control samples ($p < 0.05$). Lanes 1 to 5 and 7 were obtained from the same blot. Although Lane 6 was from a different blot, it was confirmed that the densities of the standard synthetic peptide in 2 blots were identical. unTx, untreated APP23 mice; Aβ-Fc, vaccinated mice; Aβ-pep, synthetic Aβ peptide positive control. **(C, D)** Real-time polymerase chain reaction analysis of messenger RNA (mRNA) levels of phagocytosis-related receptors, Fcγ receptor 1 (FcγR1) and scavenger receptor A (SR-A). Messenger RNA for these receptors was significantly greater in vaccinated APP mice than in untreated wild-type mice. Receptor mRNAs were also upregulated in untreated APP mice, consistent with the observations that microglia were activated and increased in untreated APP mice (Fig. 3). There were no significant differences between vaccinated and untreated APP mice or between untreated APP and wild-type mice in **(C)** and **(D).** GAPDH, glyceraldehyde-3-phosphate dehydrogenase.

(Fig. 3A) and hippocampus (Fig. 3B). In untreated APP23 transgenic mice, activated ameboid microglia were seen around amyloid plaques (periplaque area); their processes were present deep within the plaques (Fig. 3C). In areas away from the plaques (remote area), ramified microglia were similar to those in wild-type mice (Fig. 3D). After DNA vaccination, microglia in the periplaque area seem to be increased in number and were clustered around the plaques (Fig. 3E). The major difference between vaccinated and nonvaccinated AD mice, however, was the morphological change of microglia in the remote areas. In vaccinated mice, microglia had more ameboid forms with long processes (Fig. 3F). To analyze the increase of microglia in a semi-quantitative manner, microglia were counted in both peri-plaque and remote areas in brain sections from normal, untreated, and treated mice. At 9 months of age, there were significantly more microglia in both areas in treated compared with untreated AD mice ($p < 0.01$); in treated mice, microglia were more numerous in periplaque areas (40.3 ± 7.9 in each 600 × 400 μm field) compared with remote areas (30.9 ± 2.7 in each field; Fig. 3G). At 15 months of age, immunostained microglia were also more numerous, particularly in periplaque areas in AD mice, with patterns similar to those at 9 months of age (Fig. 3H).

In double-stained brain sections, small Aβ deposits seemed to be located inside microglia. This was confirmed by confocal microscopy. In periplaque area, Cy3-labeled microglia (red) (Fig. 4B) enclosed fluorescein isothiocyanate–labeled Aβ deposits (green) (Fig. 4A). The merged image indicates small Aβ deposits within microglia (arrows in Fig. 4C). Ingestion of Aβ deposits was confirmed by 3-dimensional reconstruction view. Localization of Aβ deposits within the cytoplasm of microglia was demonstrated by the

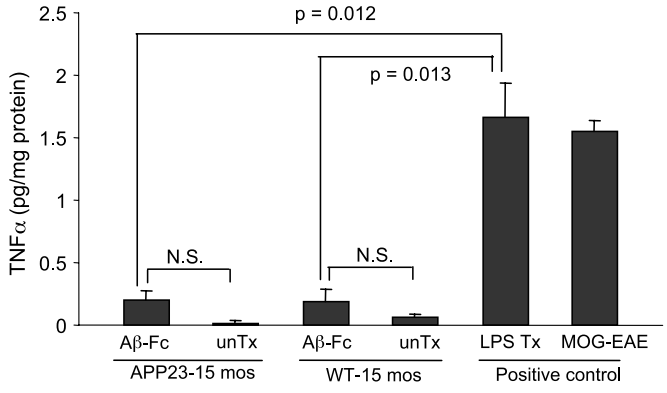

FIGURE 6. Tumor necrosis factor (TNF) levels in the brains of β-amyloid (Aβ)-Fc–treated and untreated B6 and APP23 mice detected by ELISA of CNS tissue homogenates. Large amounts of TNF were detected in the brains of positive control mice that had been given either an intraperitoneal injection of lipopolysaccharide or myelin oligodendrocyte protein (MOG)–induced experimental autoimmune encephalomyelitis ([EAE] spinal cord sample). Tumor necrosis factor in the brains of untreated B6 and APP23 mice was almost undetectable. p values are indicated. Additional p values for Aβ-Fc APP23 versus MOG-EAE and Aβ-Fc wild-type versus MOG-EAE are p = 0.0001 and p = 0003, respectively. Aβ-Fc, vaccinated mice; unTx, untreated APP23 mice.

different plane of the z axis view (Figs. 4D, E). Semi-quantitative analysis revealed that the numbers of microglia phagocytosing Aβ deposits were significantly increased in vaccine-treated compared with untreated mice ($p < 0.05$; Fig. 4F). Phagocytosis in remote areas was interpreted as indicating clearance of invisible small Aβ aggregates such as Aβ oligomers by activated microglia.

To confirm this, we performed Western blot analysis. As shown in Figures 5A and B, Aβ aggregates were reduced by DNA vaccination compared with untreated controls. Thus, Aβ phagocytosis away from amyloid plaques and Aβ oligomer reduction after DNA vaccination may be beneficial for cognitive decline in AD patients because Aβ oligomers show toxic effects on neurons in AD brains (19, 20). We also quantitated mRNA levels of phagocytosis-related receptors, Fcγ receptor 1 and scavenger receptor A, by real-time PCR. As shown in Figures 5C and D, mRNA for these receptors was significantly upregulated in vaccinated APP mice compared with untreated wild-type mice. However, receptor mRNA was also upregulated in untreated APP mice. This finding was consistent with morphological observations that microglia were activated and increased in untreated APP mice (Fig. 3).

TNF Did Not Increase Significantly in the Brain After DNA Vaccination

To determine whether activated microglia in AD mice are neurotoxic or neuroprotective, we measured the TNF levels with ELISA. Tumor necrosis factor is a proinflammatory cytokine and is regarded as a biomarker of risk for the development of meningoencephalitis (21). Large amounts of TNF were detected in the brains of LPS-treated mice and in the spinal cords of mice with MOG-induced EAE, but levels of TNF in the brain of vaccinated and control B6 and APP23 mice assayed in the same manner were very low (Fig. 6). Thus, activated microglia in the brains of DNA vaccinated AD model mice did not produce large amounts of TNF and seem to be nonneurotoxic.

Direct Effects of Anti-Aβ Antibodies on Aβ Plaques as Suggested by Amyloid Plaque Immunoreactivity Assay

The second hypothesis to explain the mechanism of Aβ reduction is the direct effect of anti-Aβ antibodies on Aβ deposits, leading to the dissolution of amyloid fibrils or neutralization of Aβ oligomers (22). Because it was difficult

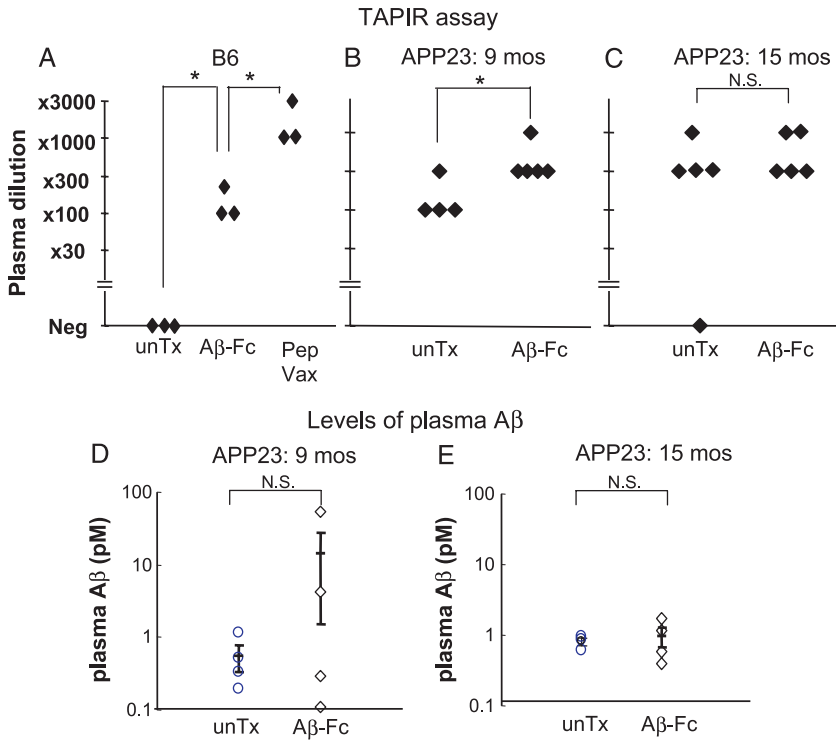

FIGURE 7. Tissue amyloid plaque immunoreactivity (TAPIR) assay and plasma β-amyloid (Aβ) levels in DNA vaccinated and untreated mice. **(A–C)** The binding of plasma from Aβ-immunized mice to Aβ plaques was determined using the TAPIR assay. **(A)** In plasma from untreated B6 mice, there was no Aβ-binding activity (unTx). By contrast, plasma from Aβ peptide–immunized B6 mice (Pep Vax) showed high titers, and plasma from DNA-vaccinated mice (DNA Vax) showed intermediate values. Asterisks indicate $p < 0.05$. **(B)** Plasma from untreated APP23 mice at 9 months of age showed intermediate binding, which was significantly different from the treated group ($p < 0.05$); differences were not significant (N.S.) at 15 months of age **(C)**. **(D, E)** At 9 months of age, plasma Aβ levels were slightly increased in some mice after DNA vaccine therapy **(D),** but at 15 months of age, plasma Aβ levels in treated mice were almost the same as those of untreated mice **(E)**. No differences between treated and untreated groups at either age were significant (N.S.). unTx, untreated APP23 mice; Aβ-Fc, vaccinated mice.

to estimate the direct effects in vivo, we measured Aβ-binding activities of plasma from treated and untreated mice using a tissue amyloid plaque immunoreactivity assay on sections from APP23 mice. First, we determined the plaque-binding ability of plasma taken from nonimmunized and immunized B6 mice (Fig. 7A). Plasma samples from non-immunized mice did not show detectable levels of amyloid plaque immunoreactivity activities, whereas samples from Aβ peptide–immunized mice showed significantly higher levels. Plasma from DNA vaccine–injected mice showed intermediate levels (Fig. 7A). The binding activity of plasma from vaccinated APP23 mice was significantly higher than that from untreated APP23 mice at 9, but not at 15, months of age (Figs. 7B, C). It should be noted that amyloid plaque immunoreactivity activities of plasma of untreated APP23 mice were elevated, especially at 15 months. This may correspond to elevation of the plasma antibody titer of untreated model mice as previously reported (7). The Aβ plaques were, however, negative for IgG in these mice (Fig. 2B). Collectively, these findings indicate that the binding activities of anti-Aβ antibodies to Aβ were augmented by DNA vaccination at early stages of the disease, but that the direct effects of antibodies are not as strong at later stages.

Plasma Aβ Levels in Vaccinated and Untreated Mice

We next measured the levels of plasma Aβ peptide to evaluate the so-called sink effect by blood-circulating anti-Aβ antibodies. At 9 months of age, plasma Aβ was slightly elevated in some cases after vaccine treatment (Fig. 7D). At 15 months of age, the levels of plasma Aβ in the treated group were almost the same as those in the untreated group (Fig. 7E). These findings suggest that Aβ efflux from the brain to blood (i.e. "peripheral sink") is present in some treated mice at an early stage, but does not seem to be the major route of Aβ reduction after DNA vaccination.

DISCUSSION

Immunotherapies against AD are effective not only in the mouse model (3, 23), but also in human clinical trials (5); however, the mechanisms by which raised or transferred anti-Aβ antibodies reduce Aβ deposition in the brain remain to be elucidated. We examined 3 possible Aβ reduction mechanisms to determine the major route of Aβ clearance in our DNA vaccination system and found that DNA vaccination enhances the phagocytosis of Aβ deposits by microglia. Because Aβ plaques in the brains of vaccinated, but not of empty vector–administered and untreated mice, were positive for IgG, an IgG-mediated immune-mediated mechanism such as Fc-mediated phagocytosis of Aβ by microglia may take place after DNA vaccination. Although it has been reported that Aβ reduction by activated microglia after glatiramer acetate treatment was achieved without the involvement of anti-Aβ antibodies (24, 25), we believe that the antibodies play an essential role in microglial activation in our DNA vaccination system. This was because plasmid DNAs containing the CpG motif without the Aβ sequence (i.e. empty vector) were not effective in Aβ reduction (Fig. 1). Increase of plaque-binding properties of plasma in vaccinated mice at 9 months of age also suggested the presence of anti-Aβ antibodies on Aβ plaques. There was, however, no significant difference in this activity between the treated and untreated groups at 15 months of age. Sink effects of plasma anti-Aβ antibodies may be present at the early stage in some treated mice but become unclear at later stages. There are at least 2 explanations for these results. First, anti-Aβ antibodies in plasma were only mildly elevated after DNA vaccination (7). Second, cerebral amyloid angiopathy may progress, especially in the late stage, and interfere with the perivascular drainage pathway of Aβ (26). Thus, microglial activation and their subsequent enhanced phagocytosis of Aβ deposits is a major Aβ clearance pathway in DNA vaccine therapy. Importantly, DNA vaccination reduced not only visible Aβ deposits, but also Aβ oligomers (Fig. 5). Thus, the findings obtained in this study provide useful information for the development of new and more effective DNA vaccines against AD.

There have been some controversies with regard to the role of microglia in AD pathogenesis. Previously, microglia were thought to be harmful and toxic to neurons in the AD brain because there were sustained inflammatory responses, including complement activation (27). β-Amyloid plaques and interferon-γ–activated microglia have synergistic effects on neuronal degeneration, which may have a role in the pathogenesis of aging and AD (28). Upon activation, microglia are known to secrete a wide variety of molecules involved in inflammation, many of which are potentially neurotoxic (29). It has been shown, however, that microglia react with Aβ plaques and phagocytose Aβ deposits under various conditions (30–33). Furthermore, activated microglia may play a protective role in the brain through the secretion of neurotrophic factors and cytokines (34). In the present study, we demonstrated that DNA vaccination induced microglial activation and augmentation of phagocytosis but did not induce large amounts of TNF production in the brains of vaccinated APP23 mice. We therefore speculate that only microglia attached to Aβ plaques may secrete TNF locally, which does not influence the level of TNF detected by ELISA, and this is less likely because microglial activation was diffuse in both periplaque and remote areas. These findings suggest that microglia after DNA vaccination may in part be neuroprotective in AD.

Increasing evidence suggests that microglia do not constitute a single uniform cell population, but rather a family of cells with diverse phenotypes—some that are beneficial and others that are destructive (35). Proper regulation of inflammatory responses to injury will arrest degeneration and promote regrowth, whereas inappropriate regulation will lead to ongoing degeneration (36). Microglial differentiation, neuroprotective or neurotoxic, might be determined by the strength of the stimulus.

The success of vaccine therapies depends on how to control microglial function to obtain beneficial effects in the AD brain. From this standpoint, DNA vaccination has advantages over other immunotherapies. The constructs of DNA vaccines can be easily manipulated by adding appropriate additional sequences to control microglial functions. Moreover, DNA vaccines may be safer because their half-life

within the body is shorter than those of others (37). If adverse side effects occur, they can be easily controlled by stopping further administration of the vaccine. Therefore, DNA vaccination may be a promising therapy for AD in the near future.

ACKNOWLEDGMENT

The authors thank Dr Matthias Staufenbiel of Novartis Institute of Biomedical Research, Nervous System, Switzerland, for critical reading of the manuscript.

REFERENCES

1. Citron M. Alzheimer's disease: Treatments in discovery and development. Nat Neurosci 2002;(suppl 5):1055–57
2. Hardy J, Allsop D. Amyloid deposition as the central event in the aetiology of Alzheimer's disease. Trends Pharmacol Sci 1991;12:383–88
3. Schenk D, Barbour R, Dunn W, et al. Immunization with amyloid-beta attenuates Alzheimer-disease-like pathology in the PDAPP mouse. Nature 1999;400:173–77
4. Orgogozo JM, Gilman S, Dartigues JF, et al. Subacute meningoencephalitis in a subset of patients with AD after Abeta42 immunization. Neurology 2003;61:46–54
5. Nicoll JA, Wilkinson D, Holmes C, Steart P, Markham H, Weller RO. Neuropathology of human Alzheimer disease after immunization with amyloid-beta peptide: A case report. Nat Med 2003;9:448–52
6. Ferrer I, Boada Rovira M, Sanchez Guerra ML, Rey MJ, Costa-Jussa F. Neuropathology and pathogenesis of encephalitis following amyloid-beta immunization in Alzheimer's disease. Brain Pathol 2004;14:11–20
7. Okura Y, Miyakoshi A, Kohyama K, Park IK, Staufenbiel M, Matsumoto Y. Nonviral Abeta DNA vaccine therapy against Alzheimer's disease: Long-term effects and safety. Proc Natl Acad Sci U S A 2006;103:9619–24
8. Morgan D. Mechanisms of A beta plaque clearance following passive A beta immunization. Neurodegener Dis 2005;2:261–66
9. Morgan D. Immunotherapy for Alzheimer's disease. J Alzheimers Dis 2006;9:425–32
10. Bard F, Barbour R, Cannon C, et al. Epitope and isotype specificities of antibodies to beta-amyloid peptide for protection against Alzheimer's disease–like neuropathology. Proc Natl Acad Sci U S A 2003;100: 2023–28
11. Bacskai BJ, Kajdasz ST, McLellan ME, et al. Non-Fc–mediated mechanisms are involved in clearance of amyloid-beta in vivo by immunotherapy. J Neurosci 2002;22:7873–78
12. Solomon B, Koppel R, Frankel D, Hanan-Aharon E. Disaggregation of Alzheimer beta-amyloid by site-directed mAb. Proc Natl Acad Sci U S A 1997;94:4109–12
13. DeMattos RB, Bales KR, Cummins DJ, Dodart JC, Paul SM, Holtzman DM. Peripheral anti-A beta antibody alters CNS and plasma A beta clearance and decreases brain A beta burden in a mouse model of Alzheimer's disease. Proc Natl Acad Sci U S A 2001;98:8850–55
14. Dodart JC, Bales KR, Gannon KS, et al. Immunization reverses memory deficits without reducing brain Abeta burden in Alzheimer's disease model. Nat Neurosci 2002;5:452–57
15. Sigurdsson EM, Scholtzova H, Mehta PD, Frangione B, Wisniewski T. Immunization with a nontoxic/nonfibrillar amyloid-beta homologous peptide reduces Alzheimer's disease–associated pathology in transgenic mice. Am J Pathol 2001;159:439–47
16. Fonte J, Miklossy J, Atwood C, Martins R. The severity of cortical Alzheimer's type changes is positively correlated with increased amyloid-beta levels: Resolubilization of amyloid-beta with transition metal ion chelators. J Alzheimers Dis 2001;3:209–19
17. Matsumoto Y, Tsukada Y, Miyakoshi A, Sakuma H, Kohyama K. C protein–induced myocarditis and subsequent dilated cardiomyopathy: Rescue from death and prevention of dilated cardiomyopathy by chemokine receptor DNA therapy. J Immunol 2004;173:3535–41
18. Matsumoto Y, Sakuma H, Miyakoshi A, et al. Characterization of relapsing autoimmune encephalomyelitis and its treatment with decoy chemokine receptor gene. J Neuroimmunol 2005;170:49–61
19. Bucciantini M, Calloni G, Chiti F, et al. Prefibrillar amyloid protein aggregates share common features of cytotoxicity. J Biol Chem 2004; 279:31374–82
20. Bucciantini M, Giannoni E, Chiti F, et al. Inherent toxicity of aggregates implies a common mechanism for protein misfolding diseases. Nature 2002;416:507–11
21. O'Toole M, Janszen DB, Slonim DK, et al. Risk factors associated with beta-amyloid (1-42) immunotherapy in preimmunization gene expression patterns of blood cells. Arch Neurol 2005;62:1531–36
22. Kotilinek LA, Bacskai B, Westerman M, et al. Reversible memory loss in a mouse transgenic model of Alzheimer's disease. J Neurosci 2002; 22:6331–35
23. Janus C, Pearson J, McLaurin J, et al. A beta peptide immunization reduces behavioural impairment and plaques in a model of Alzheimer's disease. Nature 2000;408:979–82
24. Frenkel D, Maron R, Burt DS, Weiner HL. Nasal vaccination with a proteosome-based adjuvant and glatiramer acetate clears beta-amyloid in a mouse model of Alzheimer disease. J Clin Invest 2005;115:2423–33
25. Butovsky O, Koronyo-Hamaoui M, Kunis G, et al. Glatiramer acetate fights against Alzheimer's disease by inducing dendritic-like microglia expressing insulin-like growth factor 1. Proc Natl Acad Sci U S A 2006; 103:11784–89
26. Weller RO, Massey A, Newman TA, et al. Cerebral amyloid angiopathy: Amyloid beta accumulates in putative interstitial fluid drainage pathways in Alzheimer's disease. Am J Pathol 1998;153:725–33
27. McGeer PL, McGeer EG. The inflammatory response system of brain: Implications for therapy of Alzheimer and other neurodegenerative diseases. Brain Res Brain Res Rev 1995;21:195–218
28. Meda L, Cassatella MA, Szendrei GI, et al. Activation of microglial cells by beta-amyloid protein and interferon-gamma. Nature 1995;374:647–50
29. Weldon DT, Rogers SD, Ghilardi JR, et al. Fibrillar beta-amyloid induces microglial phagocytosis, expression of inducible nitric oxide synthase, and loss of a select population of neurons in the rat CNS in vivo. J Neurosci 1998;18:2161–73
30. Wisniewski HM, Barcikowska M, Kida E. Phagocytosis of beta/A4 amyloid fibrils of the neuritic neocortical plaques. Acta Neuropathol (Berl) 1991;81:588–90
31. Rogers J, Strohmeyer R, Kovelowski CJ, Li R. Microglia and inflammatory mechanisms in the clearance of amyloid beta peptide. Glia 2002;40:260–69
32. Herber DL, Roth LM, Wilson D, et al. Time-dependent reduction in Abeta levels after intracranial LPS administration in APP transgenic mice. Exp Neurol 2004;190:245–53
33. Akiyama H, McGeer PL. Specificity of mechanisms for plaque removal after A beta immunotherapy for Alzheimer disease. Nat Med 2004;10: 117– 18; [author reply 8–9]
34. Sawada M, Imamura K, Nagatsu T. Role of cytokines in inflammatory process in Parkinson's disease. J Neural Transm Suppl 2006;(70): 373–81
35. Schwartz M, Butovsky O, Bruck W, Hanisch UK. Microglial phenotype: Is the commitment reversible? Trends Neurosci 2006;29:68–74
36. Schwartz M. Macrophages and microglia in central nervous system injury: Are they helpful or harmful? J Cereb Blood Flow Metab 2003;23: 385–94
37. Song YK, Liu F, Chu S, Liu D. Characterization of cationic liposome–mediated gene transfer in vivo by intravenous administration. Hum Gene Ther 1997;8:1585–94

